

Solvent Density and Species Dependence of the Fluorescence Stokes-Shift and Lifetime of Coumarin 152

Yoshifumi Kimura,*,# Masaki Iwasa, and Noboru Hirota

Department of Chemistry, Graduate School of Science, Kyoto University, Kyoto 606-8502

(Received May 22, 2001)

Absorption spectra, fluorescence spectra, and fluorescence lifetime of Coumarin 152 (C152) have been measured in ethane (C_2H_6), carbon dioxide (CO_2), and trifluoromethane (CF_3H) at 343 K and in CF_3H at 323 K from $\rho_r \approx 0.1$ to 2.0. The fluorescence Stokes-shift slightly decreases in C_2H_6 and CO_2 with an increase of the solvent density, while it increases up to $\rho_r \approx 0.5$ in CF_3H and remains almost constant above $\rho_r \approx 0.5$, where ρ_r is the reduced density by the solvent critical density. All these features are common to the case of C153 (Y. Kimura and N. Hirota, *J. Chem. Phys.*, **111**, 5474 (1999)). The fluorescence lifetime of C152 is found to be strongly dependent on the solvent density and temperature below $\rho_r = 1.0$ in C_2H_6. On the other hand, very large density dependence is observed in CF_3H below $\rho_r = 0.1$, although the lifetime slightly decreases with increasing the solvent density above $\rho_r = 0.1$. The fluorescence lifetime is discussed in relation with the energy difference between the S_0 and S_1 states. The quenching of the S_1 state by oxygen is also found to make a contribution to the density dependence of the fluorescence lifetime.

Various experimental and theoretical studies have been made to elucidate the molecular picture of the solvation in fluids in the medium-density region near its gas-liquid critical points.[1] Thanks to these studies, it is now evident that there is a local density enhancement effect around an attractive solute molecule in the medium-density region; i.e., the average number density of the solvent in the vicinity of the attractive solute molecule is larger than the bulk solvent density. However, we consider that there is still a gap, for example, between the local density and the absorption or fluorescence peak shift observed experimentally. For isotropic and short-ranged potential systems, several works have suggested that the spectroscopic shift can be explained by the local density.[2,3] However, for anisotropic and long-ranged systems, the situation is not so simple. We have recently found that the density dependence of solvation energy of a dipolar dumbbell solute in a dipolar dumbbell solvent cannot be explained only by the local density, since the solvation energy per solvent molecule is not a linear function of the solvent density and the solute dipole moment.[4] The solvation energy per solvent molecule is larger in the lower-density region, because in the high-density region the orientation of the solvent molecule is perturbed by the packing effect. Experimentally this kind of non-linear solvation has not yet been well-identified.

There are several problems in extracting the solvent reorganization energy (λ_S) from the analysis of the absorption and fluorescence spectra, since these spectra in fluids are often broadened by several factors. We studied the resonance Raman and the absorption spectra of a charge transfer band of Phenol Blue in various fluids; we found that there is a large decrease of the absorption bandwidth with increasing the solvent density in fluids.[5] We interpreted that this is due to the decrease of the intramolecular reorganization energy (λ_V). Recently it has been reported by several research groups including ours that the fluorescence Stokes-shift of Coumarin 153 (C153, see Scheme 1) shows quite interesting solvent density dependence in fluids.[6,7,8] We found that in argon and ethane (C_2H_6) the Stokes-shift is a decreasing function of the solvent density from $\rho_r \sim 0.7$ to 2.8, where ρ_r is the reduced density by the critical density of the solvent. The result indicates that λ_V is a decreasing function of the solvent density in these solvents. In trifluoromethane (CF_3H), the Stokes-shift is almost independent of the solvent density from $\rho_r \sim 0.5$ to 2.0, while there is a large increase up to $\rho_r \sim 0.5$. We interpreted the large Stokes-shift in the lower-density region as the results of the local density enhancement and the non-linear effect of the solvation in the low-density region. In the study, we also found that the fluorescence lifetime in CF_3H is strongly dependent on the solvent density up to $\rho_r \sim 0.1$, and that it slightly decreases with an increase of the solvent density above $\rho_r \sim 0.1$.[7] The fluorescence lifetime in C_2H_6, on the other hand, is a gradually increasing function of the solvent density up to $\rho_r \sim 1.0$. We speculated that this can be explained as in the case of 9-cyanoanthracene[9]: the change of the fluorescence lifetime is due to the change of the reaction paths; i.e., in the lower-densi-

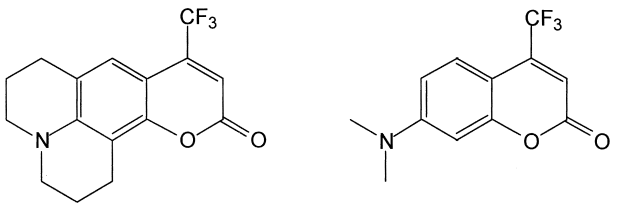

C153 C152

Scheme 1.

Present Address: International Innovation Center, Kyoto University, Kyoto 606-8501.

ty region the intersystem crossing to the T_2 state is expected to be the main path, but with an increase of the solvation to the S_1 state the T_2 state no longer remains the energy transfer path.

In this paper, we will present the study of the fluorescence Stokes-shift of another Coumarin compound (Coumarin 152 (C152), see Scheme 1) and the detailed analysis of fluorescence lifetimes of C152 and C153. The aim of the former study is to test possible effects of the molecular flexibility, and the aim of the latter is to verify the previous interpretation of the density dependence of the fluorescence lifetime. C152 is different from C153 in that the amino-group is not bridged to the aromatic group by an alkyl chain. Instead, C152 has a dimethylamino group. This makes it possible for C152 to take a twisted intramolecular charge transfer (TICT) form in the electronic excited state, although the existence of the TICT form has not been proven in the case of C152.[10] However, the molecular flexibility related to the CT process will be expected to enlarge λ_V or the Stokes-shifts. It is an interesting issue how such an effect will appear in the solvent density and species dependence of the fluorescence Stokes-shift. As is shown in the followings, although the molecular flexibility increases the absolute value of the fluorescence Stokes-shift, the solvent density dependence is not affected by this fact. As for the lifetime issue, we have made more detailed studies in this paper, including the temperature dependence, to clarify the non-radiative pathway from the S_1 state under various conditions. We have found that in C_2H_6 the apparent activation energy is largely density dependent, although that in CF_3H is not strongly dependent in the measured density region. The difference will be discussed based on the mechanism presented in the previous paper[7] in relation with the density dependence of the S_0–S_1 free energy difference (ΔG). We have also made an additional study on the effect of the molecular oxygen to the lifetime of C152 and C153, and found that the oxygen contamination contributes to the density dependence of the lifetime.

Experimental

The experimental setups for the absorption and fluorescence measurements were similar to the ones previously reported.[7] Briefly the time-dependent fluorescence spectrum was measured by a streak camera (C4334) using the doubled output of a mode-locked Ti:Sapphire laser (Coherent Mira 900-F, 100fs FWHM (full width of the half maximum), 76 MHz, 740 nm) pumped by an Ar^+ laser (Coherent Innova 300). In this study the polarization of the excitation pulse was set to the magic angle, and fluorescence was detected after the depolarization. The wavelength dependence of the time delay due to the mechanical artifact of the streak camera was corrected by using the time profile of the fluorescence of C153 in hexane, assuming no delay of the fluorescence rise at each wavelength. The wavelength calibration was done with a Hg lamp. The wavelength dependence of the sensitivity of the streak camera was corrected by measuring the reference samples (quinine, *m*-nitrodimethylaniline, and 2-aminopyridine).[11,12] The absorption spectrum was measured by a Shimadzu UV-2500 spectrometer. The high pressure optical cells used for the measurement have been described elsewhere.[5] The temperature was kept within $\pm$0.1 K at 323.2 K, $\pm$0.3 K at 343 K, and $\pm$0.5 K at 380 K by circulating thermostated water or silicon oil through the cell, and the pressure was measured by a strain gage (Kyowa PGM 500KH). The densities of fluids were calculated by empirical equations of states.[13] In measuring the absorption spectrum, the absorbance around the peak maximum was around 1.0 with the 28 mm optical path length, which corresponds to about 4×10^{-5} mol dm^{-3}. In measuring the fluorescence spectrum, the concentration was less than in the case of the absorption measurement. In the lower-density region the concentration of C152 was limited by the solubility, and was on the order of 10^{-5} mol dm^{-3} or less.

Gases of CO_2 (Sumitomo Seika, $>$ 99.98%), C_2H_6 (Sumitomo Seika, $>$ 99.0%), trifluoromethane (CF_3H) (Asahi Glass, $>$ 99.999%), and oxygen (IZUMI, 99%) were used as received. C152 and C153 (Lambda Physics) was purified by recrystallization from ethanol.

Results and Discussions

Lineshape Analysis. Figure 1 shows typical absorption ($\varepsilon(\nu)$) and fluorescence (F(ν)) spectra of C152 in C_2H_6, CO_2, and CF_3H at various solvent densities at 343 K, where ν is the wavenumber. As is shown in the figure, both absorption and fluorescence spectra show red-shifts with increasing the solvent density; the magnitude of the shift is larger in the order of C_2H_6, CO_2, and CF_3H. The spectrum also becomes structureless in the same order. To evaluate the 1st moments (ν_{abs}^{av} and ν_{fl}^{av}) of the absorption and the fluorescence lineshape functions ($g(\nu) \propto \varepsilon(\nu)/\nu$ and $f(\nu) \propto F(\nu)/\nu^3$), we used the same procedure as is described in the previous paper.[7] Briefly, the lineshape function was fitted by a sum of log-normal functions as[14]

$$h(\nu) = \sum_i h_i(\nu) \tag{1}$$

$$h_i(\nu) = \begin{cases} h_i \exp\left(-\dfrac{\ln 2}{b_i^2}[\ln(1+\alpha)]^2\right) & (\alpha > -1) \\ & (\alpha < -1) \end{cases} \tag{2}$$

where $\alpha = 2b_i^2(\nu - \nu_{P_i}) / \Delta_i$. h_i, b_i, ν_{P_i}, and Δ_i are adjustable parameters. $h(\nu)$ represents $g(\nu)$ or $f(\nu)$. This empirical equation worked well to simulate the spectrum. Typical examples of fitting are shown in Fig. 2. The dashed lines indicate components of the spectrum division by log-normal functions, and the solid lines almost overlapping with the experimental data are the sum of them. Since the decomposition of the spectrum into the sum of log-normal functions was not unique, we kept the same policy as in the case of C153: we used one main log-normal function to fit the main spectrum region including the higher-energy side of the absorption spectrum or the lower-energy side of the fluorescence spectrum to simulate the region where the experimental data were not available, and fitted the fine structure by other log-normal functions. The numbers of the log-normal functions required to fit the spectrum were as follows: in the case of the absorption spectrum: 4 for C_2H_6, 3 for CO_2, and 2 for CF_3H; in the case of the fluorescence spectrum:, 3 for C_2H_6, 2 for CO_2, and 1 for CF_3H. The 1st moment of the lineshape function was analytically calculated by the fitting parameters. The values were not strongly dependent on the decomposition of the spectrum. The estimated variation of the 1st moment is typically $\pm$70 cm^{-1}, including the experimental errors.

Figure 3 shows the solvent density dependence of ν_{abs}^{av} and ν_{fl}^{av} in all fluids at 343 K and in CF_3H at 323 K. The figure shows almost the same features as is observed in the case of

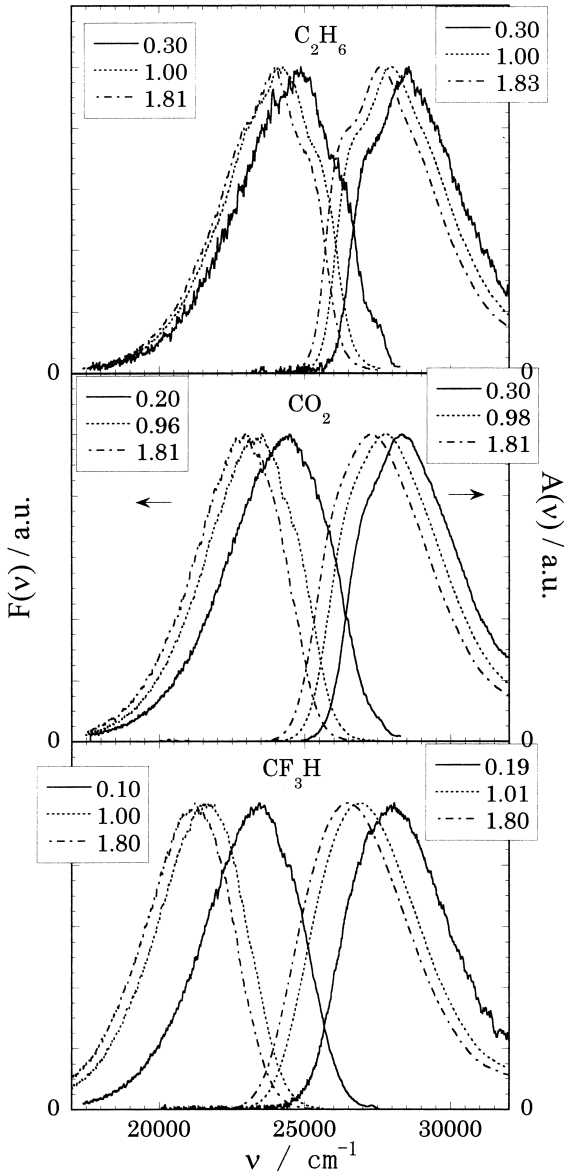

Fig. 1. Typical examples of the absorption and the fluorescence spectra of C152 in C_2H_6, CO_2, and CF_3H at various solvent densities at 343 K. The inset shows the corresponding value of ρ_r.

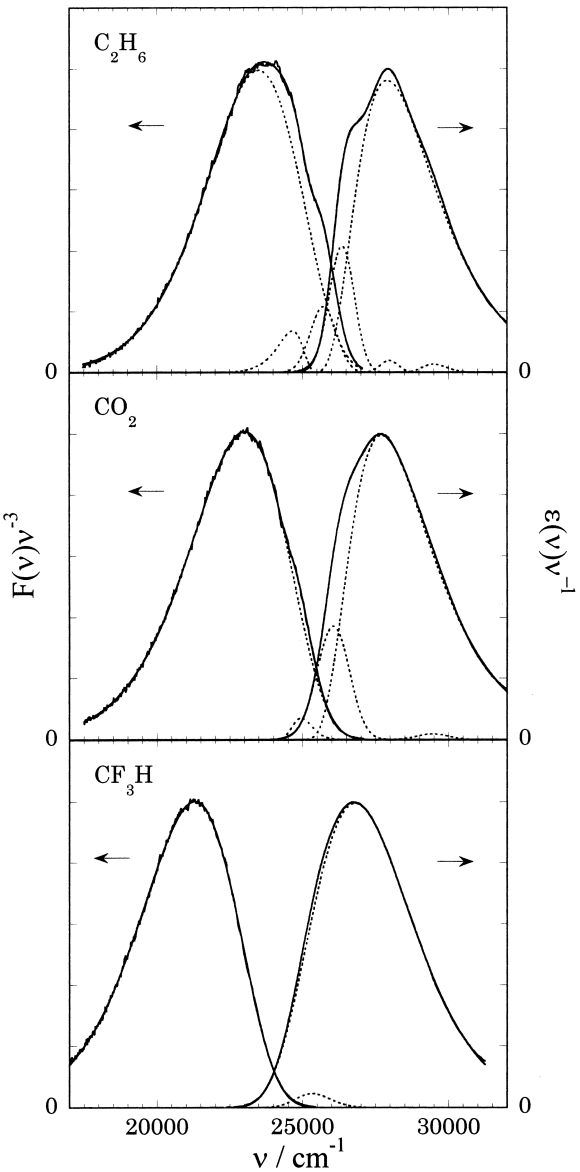

Fig. 2. The absorption and fluorescence lineshape functions in C_2H_6, CO_2, and CF_3H at 343 K and $\rho_r = 1.0$. The dashed lines in the figure show components of log-normal functions to fit the whole spectral lineshape. The sum of each component (solid line) is also shown the figure, which is totally overlapping the experimental data.

C153; i.e. the density dependence is larger in the lower-density region, and is larger in the order of C_2H_6, CO_2, and CF_3H in the low-density region. Due to the larger solubility of C152 at slightly higher temperatures than in the previous study, we can cover the lower-density region as low as $\rho_r \sim 0.2$. Since in the present study the maximum solvent density is $\rho_r = 2.0$, we cannot observe the higher density region where the density dependence of the shift becomes larger again.

Free Energy Difference and Stokes-Shift. Figure 4 shows the results of ΔG ($\equiv (\nu_{abs}{}^{av} + \nu_{fl}{}^{av})/2$) and Stokes-Shift ($\Delta\nu \equiv (\nu_{abs}{}^{av} - \nu_{fl}{}^{av})$). In the evaluation of these values, we fitted the results in Fig. 3 by a polynomial function of the solvent density as is shown in the figure, since we did not measure the absorption and the fluorescence spectra at exactly the same solvent density. Typically, the result in Fig. 4 has an error of ± 140 cm^{-1}. As is shown in Fig. 4a, in the medium-density region ($0.5 < \rho_r < 2.0$), the density dependence of ΔG is small relative to that in the lower-density region in all solvents, and the slope in the lower-density region becomes larger in the order of C_2H_6, CO_2, and CF_3H. The density dependence of ΔG at 323 K in the medium-density region in CF_3H is not different from that at 343 K.

As is shown in Fig. 4b, $\Delta\nu$ is almost constant in the medium-density region ($0.5 < \rho_r < 2.0$). More closely, $\Delta\nu$ is a slightly decreasing function of the solvent density in C_2H_6 and CO_2, and almost invariant in CF_3H. The value of $\Delta\nu$ in C_2H_6 decreases by about 150 cm^{-1} from $\rho_r \approx 0.2$ to 2.0, which is similar to the case of C153. We consider the wavy dependence in CF_3H above $\rho_r = 0.5$ at 343 K is not real, but is probably

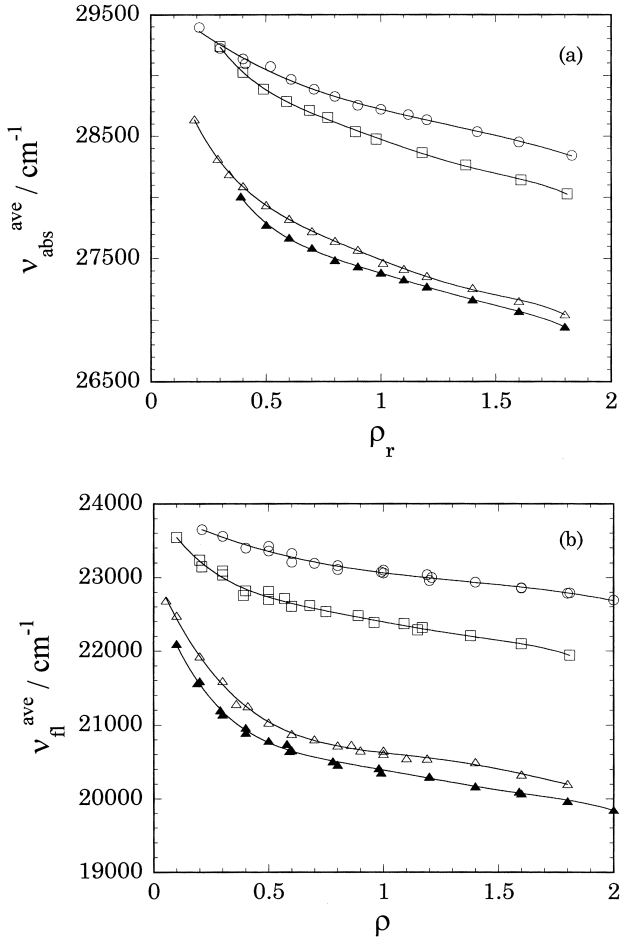

Fig. 3. The solvent density dependence of the 1st moments of the absorption (a) and the fluorescence (b) lineshape functions at 343 K (○: C_2H_6 ; □: CO_2 ; △: CF_3H) and 323 K (▲: CF_3H). The estimated variation of the 1st moment is typically ± 70 cm^{-1} including the experimental errors. The solid lines are fits to polynomial functions of ρ_r to evaluate the free energy and the Stokes shift.

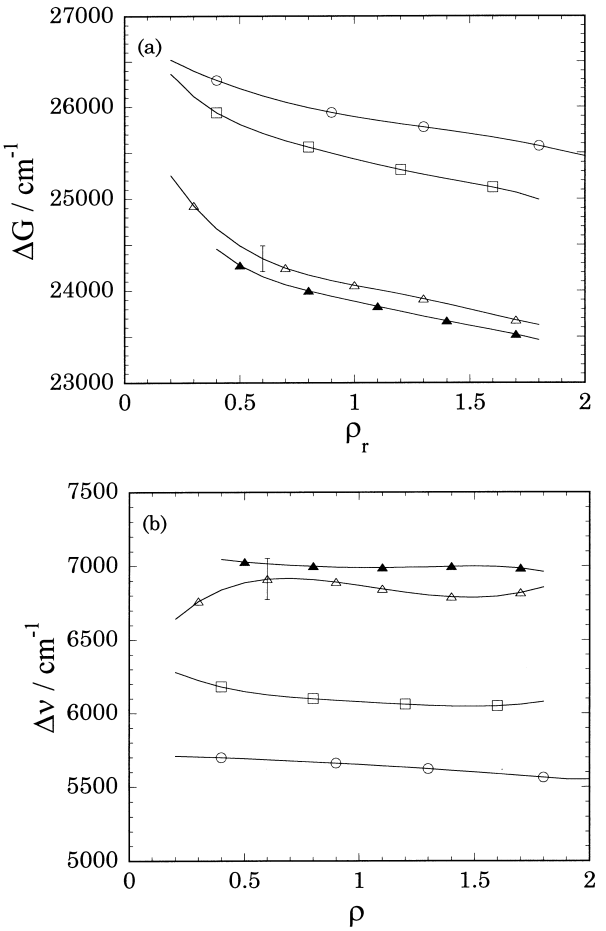

Fig. 4. The solvent density dependence of the free energy (a) and the Stokes-shift (b) at 343 K (○: C_2H_6 ; □: CO_2 ; △: CF_3H) and 323 K (▲: CF_3H). Typically the result have an error of ± 140 cm^{-1}. The values are evaluated with a step of 0.1 in ρ_r by the polynomial functions in Fig. 3 and connected by solid line.

due to the artifact from the fitting. In the present case, we can observe the low density region of CF_3H where $\Delta\nu$ decreases with decreasing the solvent density. In the low-density limits $\Delta\nu$ in different fluids should take one value. If we simply extrapolate the results in C_2H_6, the value at $\rho_r \approx 0$ is around 5750 cm^{-1}. This suggests that the large density dependence of $\Delta\nu$ is expected in the lower-density region of CO_2 and CF_3H.

The most striking features observed here are the larger density dependence of ΔG in the low-density region than in the medium- and high-density regions, the decrease of $\Delta\nu$ with increasing density in C_2H_6, and the invariance of $\Delta\nu$ above $\rho_r >$ 0.5 in CF_3H. These features are very similar to the previous observations for C153,[7] and it is evident that these are not directly related to the critical phenomena of the solvent, because the experimental temperatures are far from the critical temperature in the sense of critical phenomena. The different points between C152 and C153 are the absolute values of ΔG and $\Delta\nu$. For example, the absolute value of $\Delta\nu$ of C152 is larger than that of C153 under the same experimental condition even in C_2H_6. However, the relative difference of ΔG ($\Delta\Delta G$) between CF_3H and C_2H_6, and that of $\Delta\nu$($\Delta\Delta\nu$) are similar between the cases of C152 and C153. For example at $\rho_r = 1.6$ and 323 K, $\Delta\Delta G$ is about 2120 cm^{-1} for C153 and 2090 cm^{-1} for C152, and that $\Delta\Delta\nu$ is about 1500 cm^{-1} for C153 and 1400 cm^{-1} for C152, respectively.[15]

Considering that $\Delta\nu = 2(\lambda_S + \lambda_V)$ in a most primitive model,[7] the molecular flexibility of C152 will be expected to appear in the solvent density and species dependence of λ_V or $\Delta\nu$. If the TICT formation occurs, it is also expected that λ_S and ΔG will change largely at some experimental conditions. The similarity of the density and species dependence to C153 suggests that in a rough view the flexibility of the amino-group of C152 does not play an important role in determining the solvent density dependence of ΔG and $\Delta\nu$. According to the semiempirical MO calculations,[10] the dipole moments of the ground and excited states of C152 (μ_g and μ_e, respectively) are 6.27 D and 12.8 D, respectively, which are close to the values for C153 (6.42 D and 13.7 D, respectively). Therefore this similarity of the charge distribution both in the S_0 and S_1 states is considered to lead to a similarity of the solvent density dependence of $\Delta\nu$ and ΔG. The molecular flexibility appears in

the difference of the absolute value of $\Delta\nu$ and ΔG, which can be explained by the values without solvation, i.e., in the gaseous phase. The larger value of $\Delta\nu$ of C152 than that of C153 under the same experimental condition even in non-polar solvent such as C_2H_6 means that λ_V of C152 in the gaseous phase is larger than that of C153, probably because the molecular configuration in the excited state is more changeable due to the unbridged amino-group. On the other hand, considering the similar density and solvent species dependences of ΔG and $\Delta\nu$ mentioned in the previous paragraph again, we find it difficult to consider that some special configuration of the excited state appears under some experimental conditions of our study.

The features observed for ΔG and $\Delta\nu$ are, therefore, explained in a similar way to that of C153. The larger density dependence of ΔG is due to the local density enhancement which is commonly discussed,[1] and due to the non-linearity of the solvation energy per solvent molecule which we found recently.[4] In a similar way, the decreasing feature of $\Delta\nu$ in C_2H_6 is ascribed to the change of λ_V with the solvent density, and the invariance of $\Delta\nu$ in CF_3H is ascribed to the competition between the increase of λ_S and the decreases of λ_V with increasing the solvent density. Here we add some comments on the non-linear solvation in the low-density region. The theoretical calculation for dumbbell fluids indicates that the solvation energy per solvent molecule in the first solvation shell is quite different between high and low densities, because the orientation of the solvent molecule in the high-density fluid is affected by another solvent molecule and the solvent molecule cannot have energetically the most favorable orientation to the solute molecule in contrast to the cases of the low- and medium-density fluids which have loose solvation structure.[16,4] We consider that this non-linear solvation per solvent molecule will be much more enhanced for a real molecule, since there are several functional groups which are able to be favorable solvation sites. C152 and C153 molecules have functional groups such as carbonyl and amino groups, and it is most probable that the solvation to these sites gives a relatively large solvation energy and reorganization energy, which is demonstrated by the study on the cluster of Coumarin derivatives.[17,18]

Lifetime of S_1. The integrated fluorescence intensity decayed almost exponentially with time in all solvents studied except for the time right after the excitation, as is discussed in the previous paper.[7] The estimated lifetimes are summarized in Fig. 5. The inverted triangle at $\rho_r = 0$ is the low-density limiting value determined at 380 K as is described later. The lifetime of the fluorescence (τ_f) shows very large solvent density and species dependence in the low-density region, while τ_f slightly decreases with increasing the solvent density in the higher-density region. These results are similar to the case of C153, while in the present case we have covered the lower-density region. It is also noteworthy that the temperature dependence is quite small in CF_3H, while it is very large in the low-density region of C_2H_6.

To see the effect of the temperature at different solvent densities more clearly, we have measured the lifetime at different temperatures at three typical solvent-reduced densities (0.4, 1.0, and 1.8) in C_2H_6 and CF_3H. As is shown in Fig. 6, in CF_3H the temperature dependence is quite small in these densities, while in C_2H_6 the temperature dependence is quite different at different densities. The apparent activation energies calculated from exponential fittings to the inverse of the temperature are 1.7 kJ mol^{-1} in CF_3H at all densities, 29, 13, and 4.6 kJ mol^{-1} in C_2H_6 at $\rho_r = 0.4$, 1.0, and 1.8, respectively.

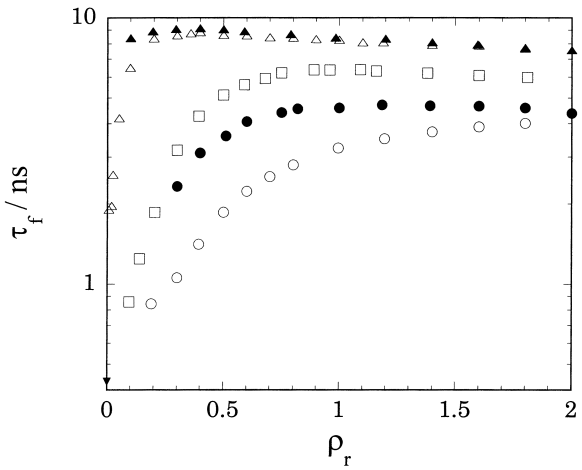

Fig. 5. The solvent density dependence of the lifetime of S_1 at 343 K (○: C_2H_6 ; □: CO_2 ; △: CF_3H) and 323 K (●: C_2H_6 ; ▲: CF_3H). The vertical axis is log-scale.

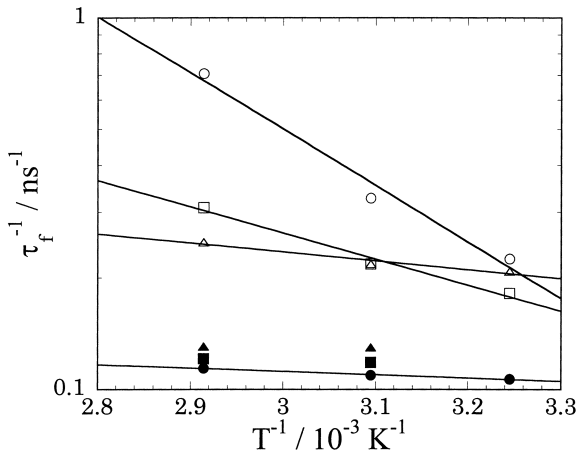

Fig. 6. The plot of τ_f^{-1} against T^{-1} at three solvent reduced densities (circle: 0.4; square: 1.0; triangle: 1.8). The open symbols are for C_2H_6 and the filled symbols are for CF_3H. The vertical axis is log-scale.

The apparent fluorescence decay rate is determined by the sum of the radiative decay rate and the non-radiative decay rate. In the previous paper we explained the density and species dependence of the fluorescence decay rate by the idea that the intersystem crossing to the triplet state is the key to understand the phenomena.[7] The study of the electronic energy level based on the semiempirical calculations suggests that a lower-lying triplet state (T_2) is close to the S_1 state, and this may provide the pathway to the non-radiative decay.[10,19] Due to the solvation to the polar S_1 state, the intersystem crossing rate to the triplet state may be reduced by lowering the energy level of the S_1 state below that of the T_2 state.

To discuss this point in more detail, we take the correlation between τ_f and ΔG. If the lowering the S_1 energy relative to the T_2 state is the key to bring the density dependence of the

lifetime, there may be a correlation between τ_f and ΔG estimated from the absorption and fluorescence spectra. The semilogarithmic plot of τ_f against ΔG is given in Fig. 7, together with the result for C153.[20,21] As is shown in the figure, a good linear relation holds between ln τ_f and ΔG above $\Delta G \sim 25800$ cm^{-1} for the case of C152. Although the correlation is not so good in the case of C153 due to the lack of the lifetime data in the lower-density region, a similar relation holds above $\Delta G \sim$ 24500 cm^{-1}. This free energy relationship suggests that the change of the energy level of S_1 is the driving force to change the rate constant in these energy regions. The different absolute values of the rates at the same ΔG in different fluids may be due to differences of the solvation to the T_2 state. The very large density dependence in the low-density region of CF_3H is due to the large solvent effect on ΔG, which exceeds the limited region of the linear free energy relation (ca.over 1300 cm^{-1}). If the solvation to the T_2 state is similar to the S_0 state, the energy difference between S_1 and T_2 for C152 is expected to be on the order of 1000 cm^{-1}.

The difference of the apparent activation energy and its density dependence between C_2H_6 and CF_3H is also qualitatively explained by the same mechanism. In the model scheme, the raise of the temperature affects the intersystem crossing rate through the change of the population distribution on the S_1 surface. The increase of energetically hot molecules in the S_1 state will accelerate the intersystem crossing rates due to the increase of the state density available in the case that the S_1 state is close to the T_2 state. On the other hand, in the case that the S_1 state is far below the T_2 state, such an effect will not be expected.

In the region of $\Delta G < 25500$ cm^{-1} there is no apparent dependence of τ_f on ΔG and the fluorescence lifetime decreases with increasing the solvent density. In the previous paper,[7] we mentioned the possibility of the fluorescence quenching due to the solvent and/or oxygen included as a contamination. To test the effect of oxygen, we made measurements on the fluorescence lifetime of C152 and C153 in pure oxygen at 380 K at various pressures. The results are shown in Fig. 8. A good linear relationship holds between the fluorescence decay rate and the oxygen pressure. The intercepts give the fluorescence decay rates in vapor as 2.3×10^{-3} ps^{-1} (τ_f = 0.43 ns) for C152 and 1.9×10^{-3} ps^{-1} (τ_f = 0.53 ns) for C153, respectively. From the slopes, the quenching rate constants for oxygen are estimated as 2.8×10 ns^{-1} MPa^{-1} for C152 and 2.7×10 ns^{-1} MPa^{-1} for C153, respectively.

Now we consider how much of oxygen is contaminated in the cell to explain the decrease of the lifetime with increasing the solvent density in the case of C152. The value of τ_f^{-1} increases from 0.11 ns^{-1} to 0.13 ns^{-1} with increasing the solvent density from 0.4 to 1.8 of ρ_r in CF_3H at 323 K. If we simply assume that this change is due to oxygen, the quenching rate due to oxygen is 0.02 ns^{-1} at ρ_r = 1.8. At ρ_r = 1.8, quenching by oxygen is considered to be diffusion limited with an efficiency of 0.2 per collision. Although the accurate value of the diffusion constant of oxygen is not known, it is expected to be on the order of 10^{-4} cm^{-2} s^{-1}.[22] Assuming the collisional diameter as 4.2 Å (using the diameters of oxygen as 3.5 Å and C152 as 4.76 Å) and the quenching efficiency as 0.2 per collision, the concentration of the oxygen is expected to be 0.3 mol m^{-3} to get the quenching rate as 0.02 ns^{-1}. This amounts to 3×10^{-3}% of the solvent molecules at ρ_r = 1.8, and this is not

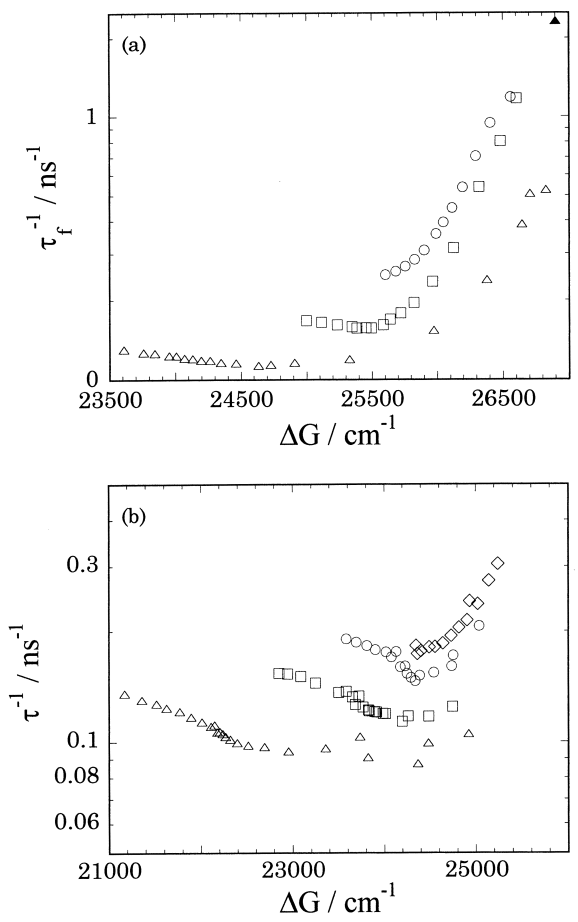

Fig. 7. The correlation between the fluorescence decay rate with ΔG for C152 (a) at 343 K (○: C_2H_6 ; □: CO_2 ; △: CF_3H), and for C153 (b) at 323 K (◇: Ar; ○: C_2H_6 ; □: CO_2 ; △: CF_3H). The filled triangle indicates the low-density limiting value estimated at 380 K.

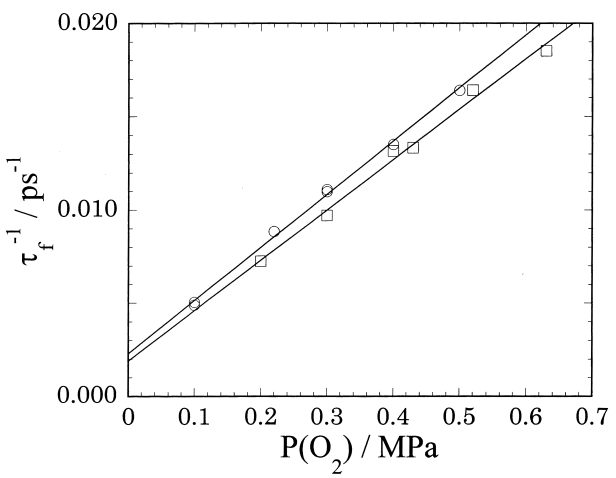

Fig. 8. The fluorescence decay rates for C152 (○) and C153 (□) at 380 K under various pressures of oxygen.

such an unrealistic value considering the purity of the solvent fluid. Therefore it is probable that the oxygen contributes the decrease of the lifetime with increasing the solvent density.

Conclusions

We have studied the solvent density dependence of the absorption and fluorescence lineshape functions, and the lifetime of the S_1 state of Coumarin 152 in C_2H_6, CO_2, and CF_3H. The results are quite similar to the case of C153, which suggests the unimportance of the non-rigidity of amino group of C152 on the density and species dependence. No explicit results were found as to the TICT formation. The density and species dependence of the fluorescence lifetime is discussed in terms of the non-radiative decay to the triple state. The fluorescence lifetime shows a good linear correlation with ΔG between the S_0 and the S_1 states above $\Delta G \sim 25800$ cm^{-1}, which indicates the decreasing the S_1 energy is the driving force to change the lifetime of the S_1 state. The temperature dependence of the fluorescence lifetime also supports the idea that, with increasing the solvent density or decreasing the energy level of S_1, the pathway of the non-radiative transition goes from the T_2 state to another state. We have also addressed the effect of the quenching by oxygen, which will explain the decrease of the fluorescence lifetime with increasing the solvent density in the higher-density region.

This work is supported by CREST (Core Research for Evolutional Science and Technology) of Japan Science and Technology Corporation (JST).

References

1 See, e.g., a) P. E. Savage, S. Gopalan, T. I. Mizan, C. J. Martino, and E. E. Brock, *AIChE J.*, **41**, 1723 (1995). b) M. Poliakoff, S. M. Howdle, and S. Kazarian, *Angew. Chem., Int. Ed. Engl.*, **34**, 1275 (1995). c) S. C. Tucker, *Chem. Rev.*, **99**, 391 (1999).

2 J. E. Adams, *J. Phys. Chem. B*, **102**, 7455 (1998).

3 S. A. Egorov, *J. Chem. Phys.*, **113**, 1950 (2000).

4 Y. Takebayashi, Y. Kimura, and M. Ohba, *J. Chem. Phys.*, **112**, 4662 (2000).

5 T. Yamaguchi, Y. Kimura, and N. Hirota, *J. Phys. Chem. A*, **101**, 9050 (1997).

6 K. Takahashi, K. Fujii, S. Saeamura, and C. Jonah, *Radiat. Phys. Chem.*, **55**, 579 (1999).

7 Y. Kimura and N. Hirota, *J. Chem. Phys.*, **111**, 5474 (1999).

8 R. Biswas, J. E. Lewis, and M. Maroncelli, *Chem. Phys. Lett.*, **310**, 485 (1999).

9 J. K. Rice, E. D. Niemeyer, and F. V. Bright, *J. Phys. Chem.*, **100**, 8499 (1996).

10 K. Rechthaler and G. Köhler, *Chem. Phys.*, **189**, 99 (1994).

11 E. Lipper, W. Nägele, I. Seibold-Blankenstein, U. Staiger, and W. Vos, *Z. Anal. Chem.*, **170**, 1 (1959).

12 W. H. Melhuish, *Appl. Opt.*, **14**, 26 (1975).

13 a) CO_2: F. H. Huang, M. H. Li, K. E. Starling, and F. T. H. Chun, *J. Chem. Eng. Jpn.*, **18**, 490 (1985). b) C_2H_6: B. A. Younglove and J. F. Ely, *J. Phys. Chem. Ref. Data*, **16**, 577 (1987). c) CF_3H : R. G. Rubio, J. A. Zolloweg, and W. B. Streett, *Ber. Bunsen-Ges. Phys. Chem.*, **93**, 791 (1989).

14 D. B. Siano and D. E. Metzler, *J. Chem. Phys.*, **51**, 1856 (1969).

15 Here we assume that $\Delta\nu$ for C152 in C_2H_6 at 323 K takes the same value at 373 K at the corresponding density.

16 Y. Kimura and Y. Yoshimura, *Mol. Phys.*, **72**, 279 (1991).

17 B. A. Pryor, P. M. Palmer, Y. Chen, and M. R. Topp, *Chem. Phys. Lett.*, **299**, 536 (1999).

18 B. A. Pryor, P. M. Palmer, P. M. Andrews, M. B. Berger, and M. R. Topp, *J. Phys. Chem. A*, **102**, 3284 (1998).

19 P. K. McCarthy and G. J. Blanchard, *J. Phys. Chem.*, **97**, 12205 (1993).

20 In order to calculate the values of ΔG in lower-density region than 0.2, we extrapolate the data in Fig. 5 to have the same intercept of 26900 cm^{-1} at $\rho_r = 0$. According to the MO calculation the energy difference is 27300 cm^{-1}.[10] Explicitly, $\Delta G(C_2H_6; \rho_r) = 26900 - 2103\rho_r + 1708\rho_r^2 - 710\rho_r^3 + 101\rho_r^4$; $\Delta G(CO_2; \rho_r) = 26900 - 3423\rho_r + 3258\rho_r^2 - 1588\rho_r^3 + 283\rho_r^4$; $\Delta G(CF_3H; \rho_r) = 26900 - 11168\rho_r + 19904\rho_r^2 - 18479\rho_r^3 + 8397\rho_r^4 - 1485\rho_r^5$. Similarly ΔG for C153 at 323 K can be fitted by the polynomial of the solvent reduced density by fixing the intercept as 25450 cm^{-1}, which is taken from Ref. 21. Explicitly, $\Delta G(Ar; \rho_r) = 25450 - 953\rho_r + 500\rho_r^2 - 219\rho_r^3 + 38\rho_r^4$; $\Delta G(C_2H_6; \rho_r) = 25450 - 2368\rho_r + 1729\rho_r^2 - 583\rho_r^3 + 66\rho_r^4$; $\Delta G(CO_2; \rho_r) = 25450 - 4280\rho_r + 4023\rho_r^2 - 1729\rho_r^3 + 256\rho_r^4$; $\Delta G(CF_3H; \rho_r) = 25450 - 10385\rho_r + 13329\rho_r^2 - 8360\rho_r^3 + 2484\rho_r^4 - 284\rho_r^5$.

21 A. Muhlpfordt, R. Schanz, N. P. Ernsting, V. Farztdinov, and S. Grimme, *PCCP*, **1**, 3209 (1999).

22 R. C. Reid, J. M. Prausnitz, and B. E. Poling, "The Properties of Gases and Liquids," 4th ed, McGraw-Hill, New York (1987).